*Quantum Electronics* **48** (8) 773–776 (2018) 

*ACOUSTO-OPTIC DIFFRACTION*

https://doi.org/10.1070/QEL16667

# Broadband acousto-optic control of the rotation velocity of the radiation polarisation vector

V.M. Kotov, E.V. Kotov

***Abstract.*** **A method is described for the formation of optical radiation with a rotating polarisation vector whose rotation frequency varies over a wide range. The method employs two identical acousto-optic (AO) modulators made of a gyrotropic crystal. The experimentally realised range of the rotation frequency of the polarisation vector of optical radiation with a wavelength of $0.6 \times 10^{-4}$ cm with the use of AO $TeO_2$ cells is found to be $\sim 6$ MHz.**

***Keywords:*** *acousto-optic diffraction, Bragg regime, rotation of the polarisation vector.*

## 1. Introduction

Acousto-optic (AO) diffraction is widely used to control the parameters of optical radiation, i.e. its intensity, phase, frequency, polarisation, propagation direction, etc. [1, 2]. A whole class of advanced AO devices is based on the use of various interference schemes, when several optical waves with different characteristics 'bump' into one another to produce a single beam. One of the interesting and promising schemes that make it possible to generate optical radiation with a rotating polarisation vector is proposed in [3], where the polarisation rotation frequency is controlled by the frequency of the acoustic wave. The idea is based on the addition of two mutually orthogonal circularly polarised waves with different frequencies. The change in the frequency of one of the waves occurs as a result of AO interaction. Experimentally, the method was realised in several stages: first, the beam of the initial radiation was split into two beams by means of AO interaction, and the radiation frequency of one of the beams shifted to the frequency of sound. Then each of the beams was passed through the phase plates to form mutually orthogonal circular polarisations, and in the last stage the beams were spatially aligned by means of beam-splitting cubes or plates. In this case, optical losses were no less than 50%.

Takahashi et al. [4] proposed another scheme, which made it possible to improve the characteristics of the device. As an AO material, a $TeO_2$ crystal was chosen, and there was no need to use phase-shifting plates, since the crystal's eigenwaves propagating near the optical axis were virtually circularly polarised. In addition, at the output of the device, circularly polarised waves were combined in a single beam by a Fresnel prism. This made it possible to reduce the optical losses practically to zero. Later, schemes were developed in which there was no need for Fresnel prisms, which significantly reduced the cost of the device as a whole [5–7]. Note that there are other ways of forming a radiation beam with a varying polarisation vector when the interference of rays is not used, and the emphasis is placed on the peculiarities of different regimes of AO diffraction. For example, Gondek and Kwiek [8] proposed a new type of a polarisation AO modulator, which permits the ellipticity of the polarisation of the light to change from 0 to 1. By varying the acoustic wave frequency and power, it is possible to vary the polarisation of light over a wide range, thereby effecting its modulation.

Rotation of the polarisation vector has already found wide application, for example, in ellipsometry [9], anemometry [10], for measuring the characteristics of birefringent fibres, determining the orientation angle of optical insulators, thicknesses and refractive indices of thin films [4], etc. The drawback of all the listed methods and devices is their high selectivity to the frequency of sound. In other words, the effective operation of devices should rely on a high stability of the sound wave frequency.

In this paper we propose a method that allows one to generate radiation with a rotating polarisation vector whose rotation frequency varies in a broad range. This significantly reduces the requirements for the stability of the frequency of sound and, at the same time, no additional adjustments are required during the frequency change process. In addition, the output radiation does not change its direction of propagation, which is very convenient when using the device in various systems, for example, for coupling radiation into optical fibres.

## 2. Formation of a rotating polarisation vector with a rotation frequency varying over a wide range

The optical scheme of the proposed method is shown in Fig. 1. Its basic elements are two identical AO modulators AO1 and AO2 made of a gyrotropic crystal. A beam of linearly polarised optical radiation $K$, incident into the first modulator, splits into two circularly polarised waves $K_1$ and $K_2$ propagating in different directions in the crystal. Modulators are controlled by rf signals of the same frequency $f$, which excite acoustic waves in the modulators. These waves propagate in modulators in strictly opposite directions. As a result of AO interaction (diffraction) in the first modulator, part of the wave $K_2$ diffracts and forms a wave $K_3$, with the frequency of the wave $K_3$ being greater than the frequency $K_2$ by an $f$. The

**V.M. Kotov, E.V. Kotov** Kotel'nikov Institute of Radio Engineering and Electronics (Fryazino Branch) Russian Academy of Sciences, pl. Akad. Vvedenskogo 1, 141190 Fryazino, Moscow region, Russia; e-mail: vmk277@ire216.msk.su

Received 20 February 2018; revision received 10 May 2018
*Kvantovaya Elektronika* **48** (8) 773–776 (2018)
Translated by I.A. Ulitkin

wave $K_1$ intersects both modulators without diffraction. The wave $K_3$, incident into the second modulator, diffracts again on the sound wave of the second modulator and forms a wave $K_4$, while the nondiffracted part $K_3$, denoted by $K_3'$, is coupled out from the modulator AO2 in a direction not coinciding with the propagation direction of the wave $K_1$. Diffraction of the wave $K_3$ in AO2 is also accompanied by an increase in the frequency of light (wave $K_4$) by an $f$. After leaving AO2, the wave $K_4$ propagates collinearly to the wave $K_1$, while the frequencies of the waves $K_1$ and $K_4$ are shifted by $2f$. Part of the radiation $K_2$, nondiffracted in AO2 (denoted by $K_2'$) is added to these waves. The diffracted part $K_3''$ propagates collinearly to $K_3'$ and does not participate in the formation of the output radiation. As a result of superposition of the waves $K_1$ and $K_4$, under the condition of equality of their amplitudes, a linearly polarised wave is formed, with the polarisation rotating with frequency $f$ [5]. To these waves, in general, the wave $K_2'$ is added, i.e. part of the wave $K_2$, which is nondiffracted in AO2 and whose frequency coincides with the frequency of the wave $K_1$. This leads to additional 'beatings' of the output signal, not related to the rotation of the polarisation vector. The higher the diffraction efficiency, the smaller the contribution of the wave $K_2'$ to the resulting radiation and the better the conditions for the rotating polarisation vector formation.

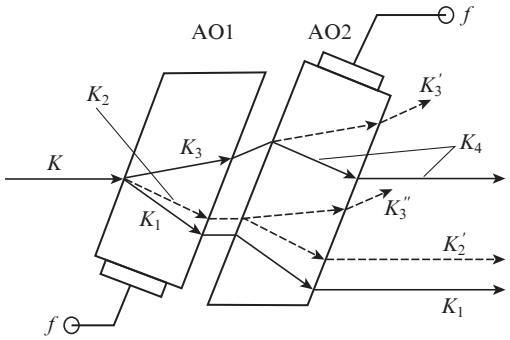


**Figure 1.** Optical scheme for the formation of radiation with a rotating polarisation vector.

Note that the scheme admits the use of both isotropic and anisotropic diffraction. However, anisotropic diffraction is of the greatest interest, since in this case it becomes possible to realise the broadband regime of the polarisation vector rotation [1].

Let AO diffraction take place in a uniaxial gyrotropic crystal, for example, in a $TeO_2$ crystal. Figure 2 shows a vector diagram of AO diffraction in a uniaxial gyrotropic crystal. The wave surface of the crystal consists of two cavities – (*1*) internal and (*2*) external. The cavities do intersect nowhere and are as close as possible only along the optical axis $Z$ of the crystal. Optical radiation with a wave vector $\boldsymbol{k}$ is incident on the crystal face $X$, oriented orthogonally to the optical axis $Z$, and decays into two eigenwaves with wave vectors $\boldsymbol{k}_1$ and $\boldsymbol{k}_2$. Only the wave $K_2$ that propagates at an angle $\alpha$ to the optical axis $Z$ participates in AO interaction. The wave vector $\boldsymbol{q}$ of sound is directed orthogonally to the $Z$ axis along the tangent to the internal cavity of the wave surface. As a result of anisotropic AO diffraction, the wave $K_2$ diffracts, forming the wave $K_3$. In the general case, diffraction is accompanied with phase mismatching. The detuning vector is denoted by $\Delta\boldsymbol{k}$ and vanishes for some value $\boldsymbol{q} = \boldsymbol{q}_0$, when the vector $\boldsymbol{k}_3$ is directed strictly along the $Z$ axis, and in the case of a significant change in $\boldsymbol{q}$ relative to $\boldsymbol{q}_0$, the vector $\Delta\boldsymbol{k}$ varies insignificantly. In Fig. 2, the range of the angle of scanning of the vector $\boldsymbol{k}_3$ is denoted by $\Theta$.

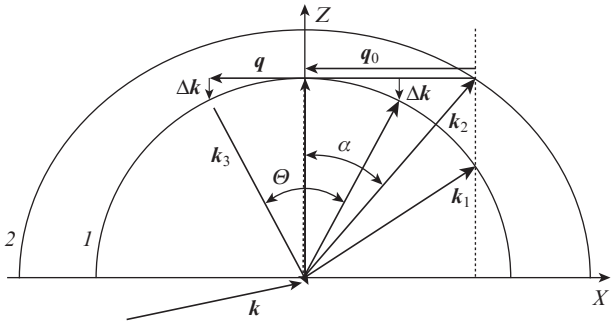


**Figure 2.** Vector diagram of AO diffraction in beam scanning mode.

To calculate the parameters of AO interaction we will use a model according to which the cavities of the wave surfaces of a uniaxial gyrotropic crystal are described by expressions

$$\frac{k_x^2}{k_o^2} + k_z^2\left[\frac{1}{k_o^2} + \left(\frac{\lambda}{2\pi}\right)^2 G_{33}\right] = 1, \tag{1}$$

$$\frac{k_x^2}{k_e^2} + k_z^2\left[\frac{1}{k_o^2} - \left(\frac{\lambda}{2\pi}\right)^2 G_{33}\right] = 1, \tag{2}$$

where Eqns (1) and (2) describe the internal and external cavities of the wave vectors, respectively; $k_x$ and $k_z$ are the lengths of the projections of the wave vector of the light propagating in the crystal along the $X$ and $Z$ axes; $k_o = 2\pi n_o/\lambda$; $k_e = 2\pi n_e/\lambda$; $\lambda$ is the wavelength of light; $n_o$ and $n_e$ are the main refractive indices of the crystal; and $G_{33}$ is a component of the pseudotensor of gyration [11]. Then from the vector diagram using relations (1), (2) it is easy to find the length of the vector $\boldsymbol{q}_0$, whence, using the relation $q_0 = 2\pi f_0/V$ ($f_0$ and $V$ are the frequency of sound and the speed of sound in the crystal), we find the frequency $f_0$, for which $\Delta\boldsymbol{k} = 0$:

$$f_0 = \frac{V}{\lambda} n_o n_e \sqrt{\frac{2G_{33}}{1 + n_o^2 G_{33}}}. \tag{3}$$

We restrict the frequency band of sound to a certain detuning value $\Delta k_0$. For a given $\Delta k_0$, the frequency band will be determined by the expression:

$$\Delta f = 2\frac{V}{\lambda} n_o \sqrt{1 - \left(\frac{k_o}{\sqrt{1 + n_o^2 G_{33}}} - \Delta k_0\right)^2 \left(\frac{1 - n_o^2 G_{33}}{k_o^2}\right)}. \tag{4}$$

Specific calculations will be carried out with for following parameters used in our experiment: $\lambda = 0.63 \times 10^{-4}$ cm, $n_o = 2.26$, $n_e = 2.41$, $G_{33} = 2.62 \times 10^{-5}$, $V = 0.617 \times 10^5$ cm s$^{-1}$. Then from (3) we obtain $f_0 = 38.6$ MHz. Let $\Delta k_0 = 1$ cm$^{-1}$. The analysis shows that this value corresponds to the maximum diffraction efficiency of 0.96. The frequency band $\Delta f$ corresponding to a given value of $\Delta k_0$ is, as is not difficult to obtain from [4], equal to $\sim 13$ MHz. From the above estimates, it can be seen that the use of AO cells made of $TeO_2$ in the scheme of Fig. 1

allows the polarisation vector of optical radiation to rotate in a wide frequency band of sound (at least 13 MHz) without additional mechanical adjustments.

We estimate the effect of the polarisation ellipticity of optical waves on the modulation depth of the resulting signal. Suppose that the optical radiation propagates along the $Z$ axis, the polarisation vector lies in the $XY$ plane, the polarisation is elliptical, and the axes of the polarisation ellipse are directed along the $X$ and $Y$ axes. Then, following the procedure of [3], the electric field components along the $X$ and $Y$ axes can be written in the generalised form as follows:

$$E_{Rx} = E_1 \cos\omega_r t, \quad E_{Ry} = -\rho_1 E_1 \sin\omega_r t \tag{5}$$

for a right-handed wave and

$$E_{Lx} = \rho_2 E_2 \cos\omega_l t, \quad E_{Ly} = E_2 \sin\omega_l t \tag{6}$$

for a left-handed wave. Here $E_{Rx}$ and $E_{Ry}$ are the components of the field of the right-handed wave; $E_1$, $\rho_1$ and $\omega_R$ are the amplitude and ellipticity of the field polarisation, as well as its cyclic frequency; $E_{Lx}$, $E_{Ly}$, $E_2$, $\rho_2$ and $\omega_L$ are the same parameters for the left-handed wave; and $t$ is time. We assume that the frequencies $\omega_R$ and $\omega_L$ differ by the cyclic frequency of the sound $\Omega$, that is, $\omega_L - \omega_R = \Omega$. The total field along the $X$ axis is:

$$\begin{aligned} E_x &= E_{Rx} + E_{Lx} = E_1 \cos\omega_R t + \rho_2 E_2 \cos\omega_L t \\ &= A_1 \cos(\omega_R + \varphi_1) t. \end{aligned} \tag{7}$$

Similarly for a field along the $Y$ axis, we have

$$\begin{aligned} E_y &= E_{Ry} + E_{Ly} = -\rho_1 E_1 \sin\omega_R t + E_2 \sin\omega_L t \\ &= A_2 \cos(\omega_R + \varphi_2) t. \end{aligned} \tag{8}$$

Here

$$\begin{aligned} A_1 &= \sqrt{E_1^2 + E_2^2\rho_2^2 + 2E_1E_2\rho_2 \cos\Omega t}\,, \\ A_2 &= \sqrt{\rho_1^2 E_1^2 + E_2^2 - 2E_1E_2\rho_1 \cos\Omega t} \end{aligned} \tag{9}$$

are the total amplitudes of the fields along the $X$ and $Y$ axes, respectively; and $\varphi_1$ and $\varphi_2$ are their phases. It is seen that when the frequency $\Omega$ is changed, the amplitude $A_1$ changes from $A_{1\max} = |E_1 + \rho_2 E_2|$ to $A_{1\min} = |E_1 - \rho_2 E_2|$. In a similar way, $A_2$ varies from $A_{2\max} = |E_2 + \rho_1 E_1|$ to $A_{2\min} = |E_2 - \rho_1 E_1|$. The depth of intensity modulation is

$$\eta = \frac{I_{\max} - I_{\min}}{I_{\max} + I_{\min}} \times 100\,\%, \tag{10}$$

where $I_{\max}$ and $I_{\min}$ are the maximum and minimum intensity values of the modulated light. In our case,

$$\eta = \frac{(E_1 + \rho_2 E_2)^2 - (E_1 - \rho_2 E_2)^2}{(E_1 + \rho_2 E_2)^2 + (E_1 - \rho_2 E_2)^2} \times 100\,\%, \tag{11}$$

the radiation is polarised along the $X$ axis; and

$$\eta = \frac{(E_2 + \rho_1 E_1)^2 - (E_2 - \rho_1 E_1)^2}{(E_2 + \rho_1 E_1)^2 + (E_2 - \rho_1 E_1)^2} \times 100\,\%, \tag{12}$$

the radiation is polarised along the $Y$ axis. The maximum modulation depth for both polarisation directions is reached at $E_1 = E_2$ and $\rho_1 = \rho_2 = \rho$:

$$\eta = \frac{2\rho}{1 + \rho^2}. \tag{13}$$

The ellipticity $\rho$ of the wave propagating in a uniaxial gyrotropic crystal at an angle $\alpha$ to the optic axis of the crystal is defined as [12]

$$\begin{aligned} \rho = \frac{1}{2G_{33}} \Bigg[ &\sqrt{\tan^4\alpha \left(\frac{1}{n_o^2} - \frac{1}{n_e^2}\right)^2 + 4G_{33}^2} \\ &- \tan^2\alpha \left(\frac{1}{n_o^2} - \frac{1}{n_e^2}\right) \Bigg], \end{aligned} \tag{14}$$

where the angle $\alpha$ is can be easily obtained from Fig. 2 when using relation (3):

$$\sin\alpha \approx q/k_o = n_e \sqrt{2G_{33}(1 + n_o^2 G_{33})^{-1}}\,. \tag{15}$$

Substituting the values for $n_o$, $n_e$, $G_{33}$ into (14) and (15), we obtain $\alpha \approx 99°$, $\rho \approx 0.8722$, and it follows from (13) that $\eta \approx 99\,\%$. In other words, in our case the ellipticity practically does not affect the modulation depth. We add that the modulation depth of the intensity of the light polarised along directions that do not coincide with the $X$ or $Y$ axis may be even larger. In this sense, the considered polarisation directions are not optimal. However, the difference in the modulation depths for any polarisation direction is so insignificant that in our case it can be neglected.

Other factors, such as insufficient diffraction efficiency and incomplete spatial alignment of interfering beams, lead to a significant decrease in the modulation depth. The first factor directly reduces the share of the rotating polarisation component, while the intensity of the nondiffracted component, the $K_2'$ wave, increases (see Fig. 1). This wave, interfering with the wave $K_4$, causes additional 'beatings' of the intensity of the output radiation, not related to polarisation rotation. In addition, the wave $K_2'$ interfering with the wave $K_1$ forms a stationary field with a nonrotating polarisation vector, which leads to an increase in the noise component. Therefore, in any case, for effective operation of the device, it is necessary to decrease the intensity of the wave $K_2'$, i.e., to increase the AO diffraction efficiency.

## 3. Experiment and discussion

To test the proposed variant, we performed an experiment. The schematic shown in Fig. 1 was taken as a basis. As the AO cells we used modulators made of a $TeO_2$ crystal measuring $1.0 \times 1.0 \times 1.0$ cm along the [110], $[1\bar{1}0]$ and [001] directions, respectively. A piezoelectric transducer made of $LiNbO_3$, which generates a transverse sound wave, was glued to the crystal face (110). The frequency ranges of the first and second modulators were, respectively, 20–35 and 25–40 MHz at a 3 dB level. The optical faces (001) were AR-coated for a wavelength of $0.63 \times 10^{-4}$ cm. The linearly polarised radiation from the He–Ne laser was passed through both modulators in full accordance with Fig. 1. Each of the modulators was individually adjusted to the diffraction regime to ensure angular scanning of the first diffraction order in a wide frequency band. The upper scanning frequency did not exceed ~35 MHz, since

at higher frequencies an efficient transfer of radiation into the second Bragg order began. After adjustment, the modulators were controlled simultaneously by one RF generator. The electric signal obtained from the generator was equal to ~10 V. The output radiation was passed through the polariser and was directed to a photodetector, the electric signal from which was fed to the oscilloscope. The polarisation rotation was verified by changing the position of the polariser. In our experiments, the sinusoidal signal on the oscilloscope screen shifted with changing the position of the polariser, which indicated the polarisation rotation. Figure 3 shows oscillograms of signals from the photodetector, observed at sound wave frequencies of 27.2 MHz (Fig. 3a) and 33.45 MHz (Fig. 3b). In tuning the generator from one frequency to another, no mechanical adjustments were made. Thus, a frequency tuning band of ~6 MHz is obtained, which is more than an order of magnitude greater than the frequency tuning range in Refs [5–7], where it did not exceed 0.5 MHz. The signal modulation depth in Fig. 3a was ~10% and 5% in Fig. 3b. We associate a small depth of modulation, first of all, with an incomplete spatial overlap of the folded optical beams at the device output, the overlap being reduced due to an increase in the displacement of one beam relative to the other with increasing frequency of sound. Estimates show that the distance between the axes of the beams, $r \approx \lambda fd/V$, where $d$ is the distance between the AO modulators, increases with increasing sound frequency. For example, for $d = 1$ cm (the condition of our experiment), $r = 0.028$ cm for $f = 27$ MHz and 0.033 cm for $f = 33$ MHz. The obtained values of $r$ are comparable with the diameter of the light beam (~0.07 cm). In addition, the small values of the modulation depth are also caused by the nonidentity of the characteristics of the AO modulators, namely, the difference in the input impedances, their amplitude–frequency characteristics, etc. However, we did not set ourselves the task of obtaining the limiting characteristics of the device: It was important for us to verify the wideband operation of the device as a whole.

Figure 3 shows that the electrical signal is noisy. This noise is caused by the noise of the photodetector path: In the absence of an optical signal on the photodetector, the electric signal on the oscilloscope is a horizontal line with the same amount of noise.

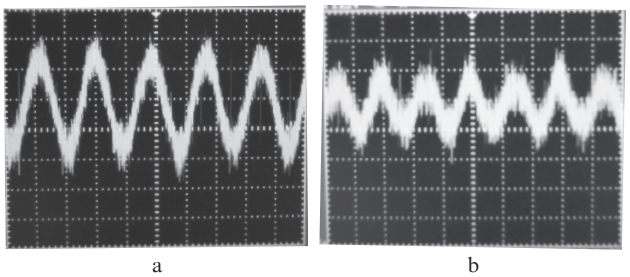


**Figure 3.** Oscillograms of electrical signals from the photodetector at sound frequencies of (a) 27.2 and (b) 33.45 MHz.

## 4. Conclusions

We have proposed a method for generating light with a rotating polarisation vector whose rotation frequency varies over a wide range. The method is based on the use of two identical acousto-optic modulators made of a gyrotropic crystal. A wide range of frequency variation is achieved by using AO diffraction in beam scanning mode.

Experiments performed with $TeO_2$ AO modulators operating in beam scanning mode have demonstrated the possibility of tuning the rotation frequency of the radiation polarisation vector with a wavelength of $0.63 \times 10^{-4}$ cm in the acoustic frequency range of ~6 MHz. At the same time, no additional mechanical adjustments were made.

The obtained results can find application in various systems which rely on the use of optical radiation with a rotating polarisation vector.

***Acknowledgements.*** The work was partially supported by the Russian Foundation for Basic Research (Grant Nos 18-07-00259 and 16-07-00064).

## References

1. Balakshy V.I., Parygin V.N., Chirkov L.E. *Fizicheskie printsypy akustooptiki* (Physical Principles of Acoustooptics) (Moscow: Radio i Svyaz', 1985).
2. Xu J., Stroud R. *Acousto-Optic Devices: Principles, Design, and Applications* (New York: John Wiley & Sons Inc., 1992).
3. Shamir J., Fainman Y. *Appl. Optics*, **21** (3), 364 (1982).
4. Takahashi H., Masuda C., Ibaraki A., Miyaji K. *IEEE Transac. Instr. Measur.*, **IM-35** (3), 349 (1986).
5. Kotov V.M., Averin S.V., Shkerdin G.N. *Quantum Electron.*, **46** (2), 179 (2016) [*Kvantovaya Elektron.*, **46** (2), 179 (2016)].
6. Kotov V.M., Averin S.V., Kotov E.V., Voronko A.I., Tikhomirov S.A. *Quantum Electron.*, **47** (2), 135 (2017) [*Kvantovaya Elektron.*, **47** (2), 135 (2017)].
7. Kotov V.M., Kotov E.V. *Opt. Zh.*, **84** (6), 51 (2017).
8. Gondek G., Kwiek P. *Ultrasonics*, **40**, 967 (2002).
9. Watkins L.R. *Appl. Opt.*, **47** (16), 2998 (2008).
10. Kotov V.M., Shkerdin G.N., Averin S.V. *VII Mezhdunarodnaya konferentsiya po fotonike i informatsionnoi optike. Sbornik nauchnykh trudov* (*V*II International Conference on Photonics and Information Optics. Collection of Scientific Papers) (Moscow: MEPhI, 2018) p. 89.
11. Sirotin Yu.I., Shaskolskaya M.P. *Osnovy kristallofiziki* (Fundamentals of Crystallophysics) (Moscow: Nauka, 1979).
12. Kotov V.M. *Akustooptika. Breggovskaya difraktsiya mnogotsvetnogo izlucheniya* (Acoustooptics. Bragg Diffraction of Multicolour Radiation) (Moscow: Yanus-K, 2016).